http://dx.doi.org/10.5935/0103-5053.20140153

*J. Braz. Chem. Soc.*, Vol. 25, No. 9, 1647-1655, 2014.
Printed in Brazil - ©2014 Sociedade Brasileira de Química
0103 - 5053 $6.00+0.00

Article

# Bacterial Cellulose as a Template for Preparation of Hydrotalcite-Like Compounds

***Gustavo F. Perotti,[a] Hernane S. Barud,[b] Sidney J. L. Ribeiro[b] and Vera R. L. Constantino*,[a]***

[a]*Departamento de Química Fundamental, Instituto de Química, Universidade de São Paulo (USP), Av. Prof. Lineu Prestes 748, 05508-000 São Paulo-SP, Brazil*

[b]*Instituto de Química de Araraquara, Universidade Estadual Paulista (UNESP), CP 355, 14801-970 Araraquara-SP, Brazil*

Celulose bacteriana (BC) foi utilizada nesse estudo como molde na preparação de compostos do tipo hidrotalcita ou hidróxidos duplos lamelares (LDHs) pelo método da co-precipitação e submetida a três tempos de envelhecimento distintos. Os compósitos isolados contendo LDH suportado na BC (BC-LDH) foram calcinados para remoção da matriz orgânica. Os óxidos metálicos mistos formados após a decomposição térmica sofreram reação de reconstrução na presença de uma solução de $Na_2CO_3$ para produzirem novamente materiais do tipo hidrotalcita (RBC-LDH). Para avaliar a influência da BC na formação do LDH, também foram analisadas as frações de LDH que não aderiram às fibras da BC e, também, o LDH sintetizado na ausência da membrana polimérica. Os difratogramas de raios X dos compósitos BC-LDH exibem picos alargados relacionados com a matriz orgânica semi-cristalina, indicando um grande nível de interação entre as fases orgânica e inorgânica. A interação também é evidenciada pelas mudanças nos perfis de decomposição dos compósitos com relação ao polímero prístino. As imagens de microscopia eletrônica de varredura mostraram a formação de partículas arredondadas submicrométricas de LDH após a remoção da membrana (RBC-LDH), diferentemente do hábito de rosetas exibido pelo LDH prístino. O envelhecimento é uma componente chave no processo de crescimento de todas as amostras de LDH produzidas, resultando na formação de partículas inorgânicas maiores à medida que o tempo aumenta. O compósito RBC-LDH envelhecido por três dias apresenta um aumento significativo na área superficial (mais do que três vezes) se comparado ao LDH preparado na ausência de BC.

Bacterial cellulose (BC) was used as a template for preparation of Hydrotalcite-type compounds or layered double hydroxides (LDHs) by co-precipitation method, and submitted to three aging times. Isolated composites containing LDH supported on BC (BC-LDH) were calcined to remove the organic matrix. Mixed metal oxides formed after thermal decomposition underwent reconstruction reaction in $Na_2CO_3$ solution producing again hydrotalcite-like materials (RBC-LDH). To evaluate the influence of BC on the LDH formation, it was also analyzed LDH fractions not attached to the BC fibers and LDH synthesized in absence of the polymeric membrane. XRD pattern of BC-LDH composites show broadened peaks related to the organic semi-crystalline matrix, indicating a deep level of interaction between organic and inorganic phases. Interaction is also evidenced by changes in the composites thermal decomposition profiles compared to pristine polymer. SEM images revealed formation of submicrometrical round-shaped LDH particles after removal of membrane (RBC-LDH), differently from the plate-habit exhibited by pristine LDH. Aging plays a key role in growth of all LDHs samples, leading to the formation of larger inorganic particles as time is increased. RBC-LDH aging for three days shows significant improvement in the surface area (more than three times) if contrasted to LDH prepared in BC absence.

**Keywords:** layered double hydroxides, bacterial cellulose, polymers, template synthesis

*e-mail: vrlconst@iq.usp.br

Dedicated to Professor Antonio Carlos Massabni on the occasion of his 70th birthday.

## Introduction

The search for nanostructured materials has become a challenge during the last decades due to some unique properties that can be achieved once such particles are obtained. These drastic changes are mainly caused by an increase in the ratio of the surface in comparison to the volume of particle which means a highest availability of reactive sites.[1] This is an especially important feature in heterogeneous catalysis field, where a large exposed surface of catalyst is beneficial to the promoted reaction, resulting in a substantial decrease in the amount of catalyst to be introduced in the system.[2]

Among the synthetic procedures available to obtain small particles, routes that originate *in situ* materials with submicrometrical dimensions, usually inserted in the "bottom-up" approach, present several advantages.[3] *In situ* assembly of nanostructures has the intrinsic ability to generate particles with a narrow distribution of both shape and size, allowing good control of the resulting product. When compared to conventional processing of larger particles, commonly assigned to "top-down" approach, synthetic methods that produce *in situ* nanoparticles possess great advantage over conventional physicochemical treatments. Particles processing may involve generation of unwanted and/or harmful residues such as in chemical treatment with strong acids and/or oxidizing agents. Notwithstanding, considerable expenses of energy and time are required in "top-down" processes such as milling and laser ablation, usually leading to particles presenting unwanted broad size dispersion.[4]

One facile way to induce the formation of submicrometrical to nanometrical particles is by introducing exogenous species in the reaction medium that are not responsible for the actual chemical reaction but can serve as support to assembly the growth of structures through non-covalent chemical interactions.[5] Organic and inorganic particles, such as membranes, rods and a wide variety of solids, can be introduced in the liquid media in order to have such function. The presence of certain functional groups as a structure-directing agents is indispensable to create an anchor point between the support and the growing crystallites and therefore, modifying its growth pattern.[6,7]

A particular case where exogenous substrates could lead to tuning the size of particles is in layered double hydroxide (LDH) systems. LDH is usually constituted by divalent and trivalent cations lying in the center of octahedral sites surrounded by hydroxyl groups, forming positively-charged sheets (Figure 1a). In order to counterbalance the layer charge arising from the presence of trivalent cations, anions occupy the interlayer domain between two adjacent sheets.[8-11] LDH is found in nature as a mineral called hydrotalcite, with chemical formula $Mg_6Al_2(OH)_{16}CO_3{\cdot}4H_2O$. The whole system can be tuned in order to produce particles with different cations in the layer structure and anions in the interlayer domain, giving rise to a broad diversity of LDHs that can be synthesized with different properties.[10,12,13]

Layered double hydroxides possesses a wide range of applications such as catalysts, fire retardants in formulations of plastics such as PVC, in drug delivery systems, ceramic precursors, as adsorbents, stabilizing agents for dyes and multipurpose anionic exchangers.[10,14-18]

The use of organic templates to create novel LDH-based structures was reported by Leroux *et al*..[19] LDH was prepared in the presence of polystyrene beads, resulting in the impregnation of the surface beads with the inorganic material. After removal of the organic fraction by either solubilization in appropriate solvent or by calcination, the remaining inorganic fraction still kept the three-dimensional network of voids surrounded by LDH particles, giving rise to a monodisperse macroporous framework.

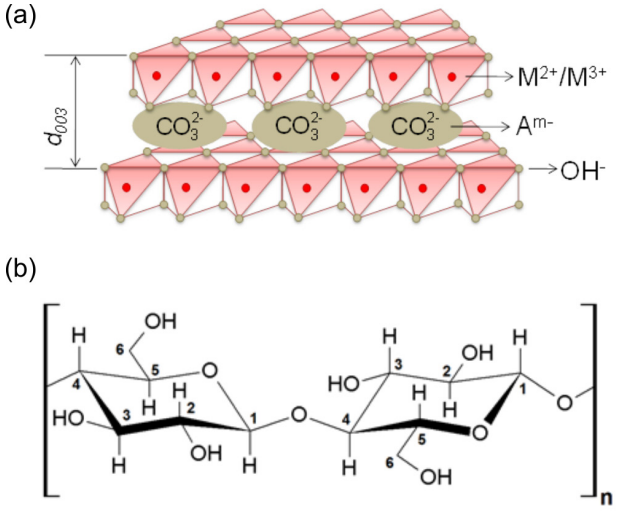


**Figure 1**. Representative structure of a layered double hydroxide (LDH) (a) and bacterial cellulose (BC) (b).

Changes in the synthetic procedures to obtain layered double hydroxides often promote modifications in the morphology of particles. This is an important feature especially in biological systems, where the shape of an exogenous particle directly reflects in the extension of its acceptance to the interior of a cell through endocytosis.[20] Furthermore, the shape factor was proven to affect not only the entrance of outside particles, but also exhibit a preferred accumulation in some specific sites along the cell. Xu *et al*.[21] synthesized LDH-based particles with different morphologies and studied the distribution of

such materials along mammalian cells. It was reported that nanorods particles, once inside the cell, are translocated to the interior of the nucleus, while nanosheets of the same material remained along the cytosol. Such approach can be used to create novel materials to interact with specific sites in living organisms, broadening the options for their use in cellular biomedicine.[21]

An interesting external agent that can be added to the reaction medium while LDHs are being synthesized is bacterial cellulose (BC). BC is a lignin free polymer obtained from *Gluconacetobacter xylinus* cultures.[22,23] When harvested under proper circumstances, this bacteria has the ability to secrete bundles of cellulose chains as part of its metabolism and therefore, allowing the production in large scale of these membranes, that can vary in thickness depending on the culture time.[24,25] As a remarkable characteristic, BC exhibits a large random net-like three dimensional network comprised of bundles of cellulose chains packed to form nanometrical ribbons.[24] Cellulose chains are formed by β-D-glucopyranose monomers containing three hydroxyl groups (Figure 1b) that can serve as a bridge for LDH nucleation. When hydrated, BC presents large pores along the whole structure,[24] resulting in a possible and vast interface for interactions and therefore, interfering in the growth pattern of the inorganic particles.[26] Barud *et al*.[27] have investigated the influence of BC in the formation of silica particles. It was found out that under certain conditions, bacterial cellulose can generate silica nanospheres ranging from 20 to 30 nm and also giving rise to completely homogeneous hybrid systems.

This work aims to use the polysaccharide bacterial cellulose as a template to synthesize LDH materials of hydrotalcite-type and evaluate the potential changes in chemical composition, structure, morphology and surface area of the LDH particles arisen from different synthetic procedures. Samples were evaluated using X-ray diffractometry (XRD), elemental chemical analysis, field emission gun scanning electron microscopy (FEG-SEM), thermogravimetric analysis (TGA) and surface area measurements (using Brunner-Emmett-Teller model). This bio-inspired route was never used before to the layered double hydroxide (LDH) synthesis.

## Experimental

### Materials

Never-dried bacterial cellulose membranes were obtained from cultures of wild strains of *Gluconacetobacter xylinus*[23] and rinsed with deionized water prior to the synthesis. Magnesium chloride ($MgCl_2 \cdot 6H_2O$), aluminum chloride ($AlCl_3 \cdot 6H_2O$), sodium carbonate ($Na_2CO_3$) and sodium hydroxide (NaOH) were purchased from Merck.

### Synthesis of layered double hydroxide-bacterial cellulose composites (BC-LDH)

BC-LDH materials were prepared using co-precipitation method[8,10] by slowly dropping a 0.25 mol $L^{-1}$ solution containing $Mg^{2+}$ and $Al^{3+}$ cations (3:1 molar ratio) to a stirred solution containing $CO_3^{2-}$ anions. This solution was previously adjusted to pH 9 and contained a $7 \times 7 \times 0.2$ $cm^3$ membrane of never dried bacterial cellulose. The system was kept at room temperature and the pH was kept between 9 and 10 during the synthetic procedure. Later, the reaction vessel was closed and the mixture was allowed to age for different periods of time under stirring (1, 3 and 6 days). Each sample was produced in different reaction vessels. After aging, the membranes were removed from the vessels, washed with deionized water and allowed to dry at room temperature for 4 days in Petri dishes. The remained solid in suspension was collected by centrifuging, washed with deionized water and dried in a desiccator containing silica-gel for 4 days.

In order to analyze the influence of bacterial cellulose on the formation of LDH particles, the same procedure to synthesize LDH was adopted in absence of the polymeric membrane. The membranes containing LDH particles were labeled as BC-LDH "X" days, with x = 1, 3 or 6. LDH samples obtained in the presence of the membrane but not attached to it were labeled as Out-LDH "X" days and the LDH formed in the absence of bacterial cellulose as LDH "X" days.

### Calcination of BC-LDH composite materials

The removal of the organic matrix was carried out by a thermal treatment in a tubular oven with continuous air flow of 50 mL $min^{-1}$ heated from room temperature to 500 °C for 2 h using a heating rate of 10 °C $min^{-1}$. After thermal treatment, samples were immediately suspended in a 0.5 mol $L^{-1}$ sodium carbonate solution for 24 h and subsequently collected by centrifuging. The isolated solid was allowed to dry in a desiccator containing silica-gel for 4 days. All the collected powder fractions from the previous synthesis (Out-LDH and LDH series) were submitted to the same thermal treatment and suspended in water containing $CO_3^{2-}$ anions to assure that any observed changes were related solely due to different synthetic conditions. The treated materials were coded with an R before the original code to represent the thermal processing and reconstruction. Therefore, samples were labeled RBC-LDH X, ROut-LDH X and RLDH X days.

### Materials characterization

XRD patterns were collected on a Rigaku Miniflex diffractometer using Cu-$K_\alpha$ radiation ($\lambda$ = 1.5451 Å) equipped with Ni filter and operating at 30 kV and 15 mA. Step size used to collect data was 0.03° and the angular domain analyzed was comprised between (2θ) 1.5 and 70°. TGA were carried out on a Netzsch STA 490 PC Luxx equipment at heating rate of 10 °C $min^{-1}$, using alumina crucible loaded with 15 mg of sample under synthetic air flow of 50 mL $min^{-1}$. The morphology of obtained materials was evaluated by field emission scanning electron microscopy (FE-SEM) on a JEOL JSM-7000F microscope (from Central Analítica of Instituto de Química da Universidade de São Paulo, IQ-USP) using uncoated samples attached to a Cu ribbon and operation tension of 1 kV. Surface area measurements (BET method) were obtained by nitrogen gas adsorption using Quantachrome Nova 1000e Surface Area equipment at a single point of $P/P_0$ = 0.32. All the samples were degassed at 150 °C for 1.25 h prior to the measurements. Mg and Al content on LDH samples were analyzed using inductively coupled plasma-atomic emission spectrometry (ICP-AES) on a Spectro Ciros CCD equipment (from Central Analítica, IQ-USP), after previous digestion of the samples with nitric acid solution. The results obtained by ICP were obtained as mean values of a duplicate.

## Results and Discussion

The X-ray diffractograms of prepared materials and pristine bacterial cellulose membrane are shown in Figure 2. The peaks are assigned to both LDH phase (non-bold numbers)[28,29] and BC phase (bold numbers).[30] Pristine bacterial cellulose exhibits two main peaks centered at (2θ) 14.5 (d = 6.1 Å) and 22.7° (d = 3.9 Å) and a shoulder at (2θ) 16.6° (d = 5.3 Å). These three signals are the contributions of two distinct crystalline phase organizations, known as $I_\alpha$ and $I_\beta$.[30-32]

During the reaction to produce the LDH material, it is expected that part of the inorganic crystals formed is anchored to hydroxyl groups present in the β-D-glucopyranose units of polymer chains through hydrogen bonds with –OH groups from LDH surface. The –OH groups from polymer can also serve as nucleation points to start the ordered growth of inorganic particles due to its interaction with $Mg^{2+}$ and $Al^{3+}$ ions in solution. In both cases, the groups of polymer main chain (both –OH and $CH_x$ groups) can affect the crystal growth of inorganic particles. Diffraction patterns obtained for BC-LDH samples present three diffraction peaks. The first peak at (2θ) 11.3° (d = 7.8 Å) is associated to the LDH

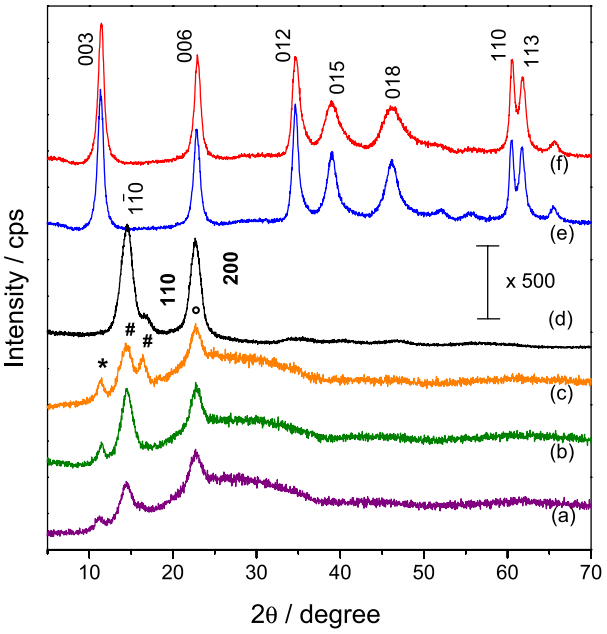


**Figure 2**. XRD patterns of BC-LDH 1 day (a), BC-LDH 3 days (b) and BC-LDH 6 days (c), pristine bacterial cellulose (d), LDH 1 day (e) and Out-LDH 1 day (f). * Denotes a peak from LDH phase. # Denotes a peak from BC phase. ° Denotes a peak with contribution of both LDH and BC phases.

phase intercalated with $CO_3^{2-}$ ions ((003) planes).[28,33] The intensity of these peaks is fairly small, possibly related to a concentration effect and also due to a decrease in the organizational level of stacking induced by bacterial cellulose during the formation of LDH layers. Diffraction patterns also present a relative broaden peak centered at (2θ) around 22.5° (d = 3.9 Å), related to both signals of crystalline structures of bacterial cellulose and the stacking plane (006) of LDH. All BC-LDH aged samples present a peak at (2θ) 14.5° (d = 6.1 Å) associated to the crystalline phases of polymer.[30,34] However, a slightly change is observed in the relative intensity of the peaks at (2θ) 14.5 and 22.7° for the BC-LDH membranes aged for longer periods, which could be caused be an increase in the signal of the amorphous region. For BC-LDH 6 days sample, a peak at (2θ) 16.4° (d = 5.4 Å) emerges where it could be seen only a shoulder in the pristine BC signal. This result could both indicate an intimate contact between both organic and inorganic phases and also a change in the ratio of crystalline structures $I_\alpha$ and $I_\beta$ due to the long contact of polymer with basic medium during aging period. XRD patterns of Out-LDH sample (Figure 2f) indicated no significant structural changes in comparison to LDH samples with the same aging time prepared in absence of BC (Figure 2e).

SEM images are shown in Figure 3. Pristine bacterial cellulose exhibits a fibrilar net-like surface, with bundles of well-packed microfibrils due to the water removal process employed. On the other side, LDH particles attached to

the membrane after 6 days of aging are presented as a fair amount of small rounded aggregates of inorganic particles. It is also noticed a considerable separation among the fibrils possibly due to some level of formation of LDH particles in deeper regions of bacterial cellulose. Out-LDH samples also presented the same rounded shape aggregates although the particle size is considerably larger than the LDH particles attached to the polymer.

Meanwhile, LDH phase is synthesized in presence of BC membrane, parts of the LDH in course of formation that are already attached to the fibrils are subject to alter its morphology due to the interaction of grown parts of particle with other sites within the anchored fibril or adjacent ones, as shown in Figure 4. It is possible to suggest that due to a size growth limitation caused by the interaction of the edges of LDH phase with BC fibrils, the formation of spherical inorganic particles is observed.

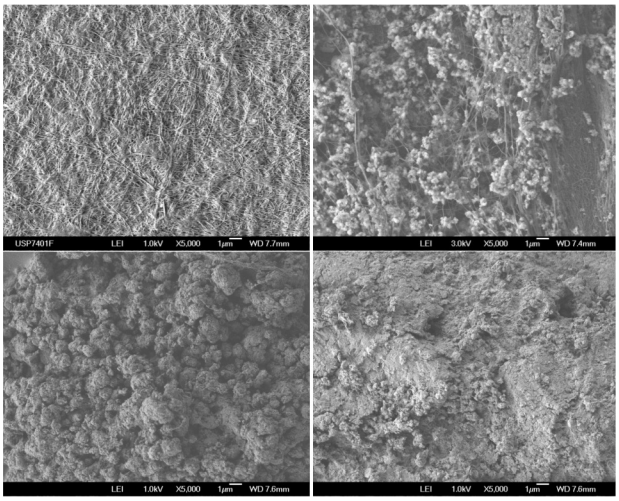

**Figure 3**. FEG-SEM images of pristine bacterial cellulose (upper left), BC-LDH 6 days (upper right), Out-BC-LDH 6 days (bottom left) and LDH 6 days (bottom right).

During the growth period of the inorganic layered structure, the average mass of part of LDH particles formed can exceed the limit that a fiber could physically hold and due to stirring used during the synthesis and through the different aging times, it can be detached and released to the aqueous medium, affecting its growth pattern and therefore, increasing their average diameter. The LDH formed in absence of BC is presented as heavily packed blocks due to the slowly drying process, forming large micrometric aggregates (Figure 3). The absence of the regular so-called *sand-rose* morphology[35] on BC-LDH samples indicates some disorientation effect of membrane in the crystallization of LDH.

TGA curves of pristine and hybrid materials are shown in Figure 5. Pristine bacterial cellulose exhibits three main


**Figure 4**. Changes in crystal growth of layered inorganic particles in contact with BC.

mass loss steps, where the first one is associated to the release of water molecules attached to the fibrils, ranging from room temperature up to 150 °C and mass loss of 6 wt.% (Figure 5a). At the temperature around 230 °C, the polymer chains of the carbohydrate start undergoing partial oxidative decomposition up to 350 °C and, as consequence, a mass loss of 58 wt.% is observed. Above this temperature, the remained char undergoes another oxidative step up to 485 °C, comprising a 36 wt.% of mass loss.[23] It is noticed a slight anticipation in the beginning of the second event of mass loss for the BC-LDH samples in comparison to pristine BC. This feature can be associated to a decrease in the interaction level of hydrogen bonds of adjacent polymer chains due to the presence of inorganic particles, as suggested by De Salvi *et al.*.[36] Based on its TGA curve profile, bacterial cellulose is a suitable support for the synthesis of LDH particles since it can be completely removed when heated up to temperatures around 500 °C.

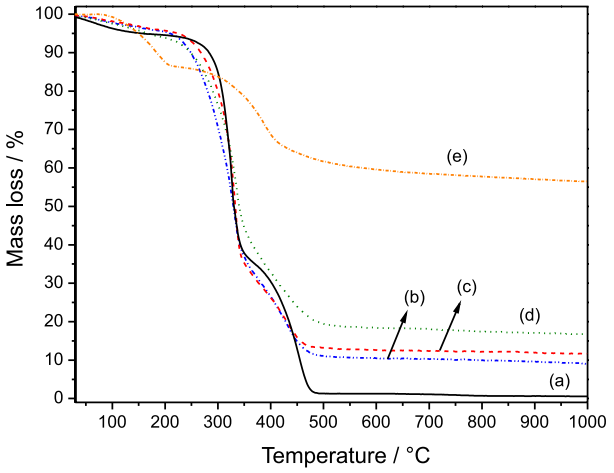


**Figure 5**. TGA curves of pristine bacterial cellulose (a), BC-LDH 1 day (b), BC-LDH 3 days (c) and BC-LDH 6 days (d) and LDH 1 day (e).

Hydrotalcite-like materials present two main steps of mass loss, as exemplified in Figure 5e. The first event is related to loss of water molecules adsorbed on the LDH platelets and also in the interlayer domain. The total water content is approximately 13.5 wt.%, whereas the temperature range associated to this mass loss occurs from room temperature up to 210 °C. In the second event, a major loss of hydroxyl groups (dehydroxilation) takes place. Release of carbonate anions in the form of $CO_2$ may also occur,[8,37] giving rise to a rocksalt structure of $Mg_6Al_2O_9$

composition at about 450-500 ºC, that is converted to a mixture of $MgAl_2O_4$ and MgO at higher temperatures.[8,11,38,39] This event starts at 220 °C (and can still occur to temperatures up to 600 °C) and presents a total mass loss of 26 wt.%. The hydrotalcite-like compounds decomposition can be represented by the following chemical equation:[39]

$$[Mg_6Al_2(OH)_{16}]CO_3.xH_2O(s) \rightarrow Mg_6Al_2O_9(s) + CO_2(g) + (8+x)\ H_2O(g)$$
$$Mg_6Al_2O_9(s) \rightarrow 5\ MgO(s) + MgAl_2O_4(s)$$

TGA curves of BC-LDH composites (Figures 5b-d) show two major differences in relation to pristine bacterial cellulose. The inorganic particles tend to slightly lower the first oxidative decomposition step of polymer and also change the profile of the second step of mass loss of the carbohydrate, indicating a close interaction between both phases. These results corroborate the proposition of hydroxyl groups from polymeric chains acting as nucleating sites for the LDH particles to grow along its net-like structure.

LDH containing especially $Mg^{2+}$ and $Al^{3+}$ cations present a unique feature named "memory effect" that allows the regeneration of its original structure after thermal treatment up to about 500 °C. After dehydration and decomposition of the anions present in the interlayer domain, the product of the topotactic decomposition of LDH (the unstable rocksalt $Mg_6Al_2O_9$) can be converted to LDH if added to water or an aqueous solution containing anions, or just kept in contact with air. The brucite-like layered structure is regenerated in a process known as reconstruction reaction.[39-41]

XRD patterns of heat treated and rehydrated LDHs are shown in Figures 6a-c (RBC-LDH) and 6d (RLDH). RLDH 3 days sample was fully restored to its original crystalline structure after employing the previously described procedure. It also applies to all the recovered LDHs that were once attached to the membrane (RBC-LDH), matching the same peak positions with LDH intercalated with carbonate anions.

All recovered samples from RBC-LDH series present also three sharp peaks at (2θ) 31.6 (d = 2.8 Å), 45.3 (d = 2.0 Å) and 56.3° (d = 1.6 Å). These peaks are associated to a small amount of NaCl phase[42] carried onto BC membrane during LDH synthesis and was not fully removed during washing process. It is also noticed that time plays a major role to stabilize more crystalline particles when layered double hydroxides are synthesized.

The recovered LDH that was aged for only one day (Figure 6a) presents all peaks associated to a regular LDH phase intercalated with carbonate anions but its signal is

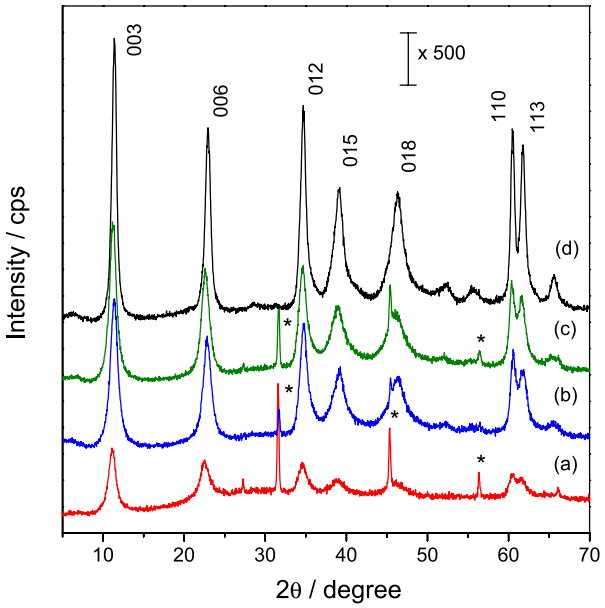


**Figure 6**. XRD patterns of RBC-LDH 1 day (a), RBC-LDH 3 days (b) and RBC-LDH 6 days (c) and RLDH 3 days (d). * NaCl.

fairly low intense when compared to other materials aged for longer times (Figures 6b-c). It means that the system obtained in this case presents less crystalline organization and could lead to particles with greater surface area due to lack of a major organization.[43] On the other hand, when LDH particles in solution are allowed to age for longer periods of time, partial solubilization of LDH particles and growth of previous existing ones lead to a better accommodation of all species over the layer. As result, it yields a well-packed structure and, hence, increases the signal obtained in XRD, although commonly originating particles with lower surface areas.[43]

**Table 1.** $Mg^{2+}$:$Al^{3+}$ molar ratios of BC-LDH series and RBC-LDH series

| Sample | $Mg^{2+}/Al^{3+}$ molar ratio |
|---|---|
| BC-LDH 1 day | 2.83 |
| BC-LDH 6 days | 2.34 |
| RBC-LDH 1 day | 2.74 |
| RBC-LDH 6 days | 2.60 |

Table 1 shows $Mg^{2+}$ to $Al^{3+}$ molar ratio for LDH particles that were attached to the membrane (BC-LDH series) and after thermal treatment and reconstruction in carbonate solution (RBC-LDH series). Samples aged for short periods tend to stabilize the LDH phase closer to the expected ratio (3:1). Late calcination and reconstruction of inorganic particles presents no significant changes on divalent to trivalent molar ratio of cations at low aging times. However, after six days of aging, both presence of polymer and thermal-reconstruction treatment influence the

ratio of cations on the final LDH. In the case of BC-LDH series, a decrease in $M^{II}/M^{III}$ ratio is possibly caused by changes in the pH of the medium due to the changes in degree of polymerization and structural organization,[44] causing a partial release of $Mg^{2+}$ from the layers and stabilizing an inorganic phase with lesser content of $M^{II}$. Also, the Ostwald ripening, a phenomenon where the equilibrium between dissolution of previously formed crystallites and incorporation of aqueous ions onto the same partially dissolved particle or a different one[45] can be responsible to alter the ratio between the metal cations in the layer. On the other hand, when the calcined BC-LDH 6 days is allowed to be reconstructed leaving it in contact with a sodium carbonate solution, the resulting RBC-LDH 6 days presents the $M^{II}/M^{III}$ ratio increased to values closer to 3, as found in nature for the mineral hydrotalcite.[8]

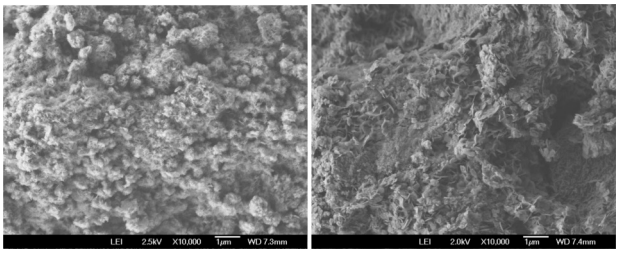

**Figure 7**. FEG-SEM images of RBC-LDH 3 days (left) and RLDH 3 days (right).

The SEM images of post-thermally treated and reconstructed LDHs are shown in Figure 7. Even after all previous treatment applied, RBC-LDH samples that were once attached to the membrane still holds a rounded shape aggregates, some of them found below submicrometric levels. Therefore, even after thermal treatment and reconstruction of LDH phase, samples still hold major morphology changes, indicating the deep influence of polymer during the assembly process of inorganic layers. Despite this particularly round-shaped aggregated formed, it can still be noticed that all RBC-LDH series also possess the same *sand-rose*[35] features as shows the SEM images of the sample R-LDH 3 days. However, the sample RBC-LDH 3 days presents smaller particles sizes than sample R-LDH 3 days but also show thinner and twisted platelets, indicating a lesser tendency of a close-packed structure than conventionally synthesized LDH. Comparing the results obtained from the RBC-LDH series, one can conclude that not only the aging time influences the size of the particles but the presence of membrane during the synthesis also has a contributive effect.

Surface area data of RBC-LDH and R-LDH samples are shown in Figure 8. The data of RBC-LDH 1 day sample was not obtained due to the very low amount of material

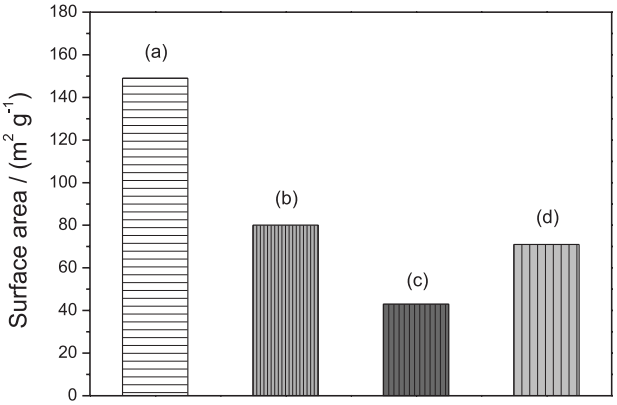


**Figure 8.** Surface area of RBC-LDH 3 days (a), RBC-LDH 6 days (b), RLDH 3 days (c) and RLDH 6 days (d).

recovered from the thermal treatment process. For LDH prepared in the absence of membrane, the obtained values of surface area are 43 and 71 $m^2 g^{-1}$ for RLDH 3 and 6 days, respectively. Although these results are in agreement with the literature[8,46] it was expected that the surface area of the less aged LDH should be higher than the most aged one. This was expected since when LDH are allowed to age, the dissolution and crystal growth of inorganic particles would help to form larger well-packed structures in comparison to less aged samples. Surface area of LDH particles is aging-dependant[33,41] and also the contributive effect of the presence of the membrane in the reaction medium should be taken in consideration. RBC-LDH samples aged for 3 and 6 days present values of surface area equal to 149 and 80 $m^2 g^{-1}$, respectively, illustrating the aging influence in the surface area values, as mentioned before. RBC-LDH 3 days sample presents almost 3.5 times higher surface area values than R-LDH 3 days sample and over 2 times the surface of R-LDH 6 days sample, showing that the polymer play a key role to avoid a dense packing of the inorganic layers, increasing the free volume among tactoids, causing an increase in the surface area. Even though the polymer is able to modify the LDH particle packing, when the period of time applied during the synthesis is long, Ostwald ripening mechanism might change the initial packing of the crystallites induced by the presence of the polymer, yielding at the end of longer times particles that resemble the ones originated in the absence of polymer. Hence, samples RBC-LDH 6 days and RLDH 6 days present similar surface area values.

## Conclusions

Composite materials comprised of bacterial cellulose and layered double hydroxides containing $Mg^{2+}$ and $Al^{3+}$ intercalated with $CO_3^{2-}$ were successfully prepared using co-precipitation method. The strong interaction between

both phases can be noticed through significant changes in XRD patterns, TGA profiles and SEM images obtained for composites in comparison to pristine BC and LDH.

According to XRD data, the intensity of peaks associated to crystalline phases of BC are altered in the presence of LDH, indicating a level of interaction that surpass the surface of the fibrils and might occur in the sub-fibril depth. Once the membrane was removed and the LDH structure was restored, it was possible to see the peaks associated to the layered phase.

SEM images also revealed that the presence of BC alters the shape when LDH particles were prepared. Instead of obtaining the regular micrometric layered aggregates, inorganic phase when prepared in presence of polymer was seen as submicrometric rounded aggregates adhered to the fibrils of BC. After the thermal removal of BC and reconstruction of LDH structure, particles still remained with original rounded shape, indicating that this polymer acted effectively as a structured directing agent.

The surface area of the particles were also evaluated and noticed that both presence of BC and aging time affected extensively over the obtained values. For longer periods of aging, it was found that particles tend to originate well-packed structures, leading to overall particles with small surface area values. On the other hand, the presence of BC membrane tends to create small rounded aggregates which lead to poor packing in comparison to LDH formed in absence of polymer, increasing the exposed surface.

## Acknowledgements

The authors acknowledge the Brazilian agencies FAPESP (2011/50318-1) and CNPq (140417/2008-7) for financial support and fellowships, and PhD Flavio M. Vichi (IQ-USP) for the surface area measurements. We also thank the NAP-NN (Núcleo de Apoio à Pesquisa em Nanossistemas e Nanotecnologia) from Universidade de São Paulo. The authors are indebted to PhD Erick Bastos (IQ-USP) by the cover image design.

## References

1. Roduner, E.; *Chem. Soc. Rev.* **2006**, *35*, 583.
2. Narayanan, R.; El-Sayed, M. A.; *J. Phys. Chem. B* **2005**, *109*, 12663.
3. Cao, G.; Wang, Y. In *Nanostructures and Nanomaterials: Synthesis, Properties and Applications*; Cao, G.; Wang, Y., eds.; World Scientific: London, UK, 2004, ch. 1.
4. Chen, C. K.; Singh, A. K.; *Org. Process Res. Dev*. **2001**, *5*, 508.
5. Ikkala, O.; Brinke, G.; *Science* **2002**, *295*, 2407.
6. Xia, H. B.; Liu, X. Y.; Zhang, K. Q.; *Chem. Mater.* **2008**, *20*, 2432.
7. Simancas, R.; Dari, D.; Velamazán, N.; Navarro, M. T.; Cantín, A.; Jordá, J. L.; Sastre, G.; Corma, A.; Rey, F.; *Science* **2010**, *330*, 1219.
8. Constantino, V. R. L.; Pinnavaia, T. J.; *Inorg. Chem.***1995**, *34*, 883.
9. Costantino, U.; Marmottini, F.; Nocchetti, M.; Vivani, R.; *Eur. J. Inorg. Chem.* **1998**, *10*, 1439.
10. Cavani, F.; Trifirò, F.; Vaccari, A.; *Catal. Today* **1991**, *11*, 173.
11. Rives, V.; *Mater. Chem. Phys.* **2002**, *75*, 19.
12. Rives, V.; Ulibarri, M. A.; *Coord. Chem. Rev.* **1999**, *181*, 61.
13. Khan, A. I.; O'Hare, D.; *J. Mater. Chem.* **2002**, *12*, 3191.
14. Evans, D. G.; Duan, X.; *Chem. Commun.* **2006**, 485.
15. Crepaldi, E. L.; Valim, J. B.; *Quim. Nova* **1998**, *21*, 300.
16. Braterman, P. S.; Xu, Z. P.; Yarberry, F. In *Handbook of Layered Materials*; Auerbach, S. M.; Carrado, K. A.; Dutta, P. K., eds.; Taylor & Francis: London, UK, 2004, ch. 8.
17. Cunha, V. R. R.; Ferreira, A. M. C.; Valim, J. B.; Tronto, J.; Constantino, V. R. L.; *Quim. Nova* **2010**, *33*, 159.
18. Cunha, V. R. R.; Petersen, P. A. D.; Gonçalves, M. B.; Petrilli, H. M.; Taviot-Gueho, C.; Leroux, F.; Temperini, M. L. A.; Constantino, V. R. L.; *Chem. Mater.* **2012**, *24*, 1415.
19. Geráud, E.; Prévot, V.; Leroux, F.; *J. Phys. Chem. Solids* **2006**, *67*, 903.
20. Sharma, G.; Valenta, D. T.; Altman, Y.; Harvey, S.; Xie, H.; Mitragotri, S.; Smith, J. W.; *J. Control. Release* **2010**, *147***,** 408.
21. Xu, Z. P.; Niebert, M.; Porazik, K.; Walker, T. L.; Cooper, H. M.; Middleberg, A. P.; Gray, P. P.; Bartlett, P. F.; Lu, G. Q.; *J. Control. Release* **2008**, *130*, 86.
22. Hestrin, S.; Schramm, M.; *Biochem. J.* **1954**, *58*, 345.
23. Iguchi, M.; Yamanaka, S.; Budhiono, A.; *J. Mater. Sci.* **2000**, *35*, 261.
24. Klemm, D.; Heublein, B.; Fink, H. P.; Bohn, A.; *Angew. Chem. Int. Edit.* **2005**, *44*, 3358.
25. Czaja, W.; Krystynowicz, A.; Bielecki, S.; Brown Jr., R. M.; *Biomaterials* **2006**, *27*, 145.
26. Yano, H.; Sugiyama, J.; Nakagaito, A. N.; Nogi, M.; Matsuura, T.; Hikita, M.; Handa, K.; *Adv. Mater.* **2005**, *17*, 153.
27. Barud, H. S.; Assunção, R. M. N.; Martines, M. A. U.; Dexpert-Ghys, J.; Marques, R. F. C.; Messaddeq, Y.; Ribeiro, S. J. L.; *J. Sol-Gel Sci. Technol.* **2008**, *46*, 363.
28. Barbosa, C. A. S.; Dias, P. M.; Ferreira, A. M. C.; Constantino, V. R. L.; *Appl. Clay Sci.* **2005**, *28*, 147.
29. Barbosa, C. A. S.; Ferreira, A. M. C.; Constantino, V. R. L.; *Eur. J. Inorg. Chem.* **2005**, *8*, 1577.
30. Czaja, W.; Romanovicz, D.; Brown Jr., R. M.; *Cellulose* **2004**, *11*, 403.
31. Nishiyama, N.; Sugiyama, J.; Chanzy, H.; Langan, P.; *J. Am. Chem. Soc.* **2003**, *125*, 14300.
32. Perotti, G. F.; Barud, H. S.; Messaddeq, Y.; Ribeiro, S. J. L.; Constantino, V. R. L.; *Polymer* **2011**, *52*, 157.

33. Fetter, G.; Hernández, F.; Maubert, A. M.; Lara, V. H.; Bosch, P.; *J. Porous Mater.* **1997**, *4*, 27.
34. Atalla, R. H.; Vanderhart, D. L.; *Science* **1984**, *223*, 283.
35. Leroux, F.; Besse, J. P.; *Chem. Mater.* **2001**, *13*, 3507.
36. De Salvi, D. T. B.; Barud, H. S.; Caiut, J. M. A.; Messaddeq, Y.; Ribeiro, S. J. L.; *J. Sol-Gel Sci. Technol.* **2012**, *63*, 211.
37. Reichle, W. T.; *J. Catal.* **1985**, *94*, 547.
38. Rebours, B.; d'Espinose de la Caillerie, J.-P.; Clause, O.; *J. Am. Chem. Soc.* **1994**, *116*, 1707.
39. Radha, A. V.; Thomas, G. S.; Kamath, P. V.; Shivakumara, C.; *J. Phys. Chem. B* **2007**, *111*, 3384.
40. Miyata, S.; *Clays Clay Miner.* **1980**, *28*, 50.
41. Xu, Z. P.; Lu, G. Q.; *Chem. Mater.* **2005**, *17*, 1055.
42. JCPDS file number 05-0628, JCPDS International Center for Diffraction Data.
43. Zhao, Y.; Li, F.; Zhang, R.; Evans, D. G.; Duan, X.; *Chem. Mater.* **2002**, *14*, 4286.
44. Shibazaki, H.; Kuga, S.; Okano, T.; *Cellulose* **1997**, *4*, 75.
45. Panda, H. S.; Srivastava, R.; Bahadur, D.; *Bull. Mater. Sci.* **2011**, *34*, 1599.
46. Bellotto, M.; Rebours, B.; Clause, O.; Lynch, J.; Bazin, D.; Elkaïm, E.; *J. Phys. Chem.* **1996**, *100*, 8535.

*Submitted on: March 10, 2014*
*Published online: July 1, 2014*

**FAPESP has sponsored the publication of this article.**